Parameter Optimization and Thermal Simulation in Laser Joining of Coach Peel Panels of Dissimilar Materials

Masoud Mohammadpour, Blair Carlson, Radovan Kovacevic

Abstract—The quality of laser welded-brazed (LWB) joints were strongly dependent on the main process parameters, therefore the effect of laser power (3.2–4 kW), welding speed (60–80 mm/s) and wire feed rate (70–90 mm/s) on mechanical strength and surface roughness were investigated in this study. The comprehensive optimization process by means of response surface methodology (RSM) and desirability function was used for multi-criteria optimization. The experiments were planned based on Box– Behnken design implementing linear and quadratic polynomial equations for predicting the desired output properties. Finally, validation experiments were conducted on an optimized process condition which exhibited good agreement between the predicted and experimental results. AlSi3Mn1 was selected as the filler material for joining aluminum alloy 6022 and hot-dip galvanized steel in coach peel configuration. The high scanning speed could control the thickness of IMC as thin as 5 µm. The thermal simulations of joining process were conducted by the Finite Element Method (FEM), and results were validated through experimental data. The Fe/Al interfacial thermal history evidenced that the duration of critical temperature range (700–900 °C) in this high scanning speed process was less than 1 s. This short interaction time leads to the formation of reaction-control IMC layer instead of diffusion-control mechanisms.

Keywords—Laser welding-brazing, finite element, response surface methodology, multi-response optimization, cross-beam laser

I. INTRODUCTION

THE global concerns about the environmental issues compelled different industries like automotive, rail car, and aerospace to fabricate products with lighter weight. Implementing lightweight materials such as aluminum, titanium, and magnesium could be the best candidates to decrease the weight of structures. From other side, using merely lightweight materials in final product is not acceptable from mechanical and economical perspectives; therefore, hybrid structures have been presented as an efficient way to satisfy these requirements [1]. Recently several attempts have been made to make hybrid parts in automotive industry for the sake of weight reduction. Yao et al. [2] mentioned that for structural parts such as A-pillars, B-pillars, and roof rails hardened steels are used and lightweight materials are

Masoud Mohammadpour is PhD candidate in Research Center for Advanced Manufacturing (RCAM), Southern Methodist University, Dallas, TX (e-mail: mohammadpour@smu.edu).
Radovan Kovacevic is Professor and director of RCAM, Southern Methodist University, Dallas, TX (e-mail: kovacevi@lyle.smu.edu).
Blair Carlson is PhD of materials science and lab group manager in General Motors Company, Manufacturing system research, Detroit, Michigan (e-mail: blair.carlson@gm.com).

employed in front and rear fenders, hood, and trunk. The existence of a significant difference between Al and steel makes the welding of them as a difficult task or even impossible due to the formation of intermetallic layers [3]. The possible IMC layers that could generate at the Fe/Al interface during the rapid heat and cooling processes are FeAl, $FeAl_3$, Fe_2Al_5, and Fe_3Al [4]. The hardness of the undesirable brittle intermetallic compounds (IMCs) was around 1000 Vickers as reported by Rathod and Katsuna [5]. The correlation between the growth of the IMC layer and thermal cycle at the Fe/Al interface was studied by Schubert et al. [6]. They showed that, by modifying the heat input, the diffusion process in dissimilar materials laser welding could control and the formation of IMC layer can be restricted. The thicker Fe-and-Al-rich intermetallic layers could jeopardize the mechanical performance of joints and could even lead to the brittle fracture. Lin et al. [7] stated that, to avoid brittle fracture, the thickness of IMC layer should be less than 10 µm. Laser-based joining processes with the capability of reaching high scanning speed could be an appropriate method for joining dissimilar materials. Several studies have been conducted on laser welding-brazing (LWB) of steel to aluminum in different joint configurations. Filliard et al. [8] investigated LWB of steel to aluminum in coach peel configuration by means of single laser beam. They succeeded to obtain joints with mechanical strength of 101% of mechanical properties of filler material and IMC layers with thickness less than 2 µm. Mohammadpour et al. [9] investigated the effect of dual-laser beam arrangement on dissimilar LWB joints in the coach peel configuration. Based upon the comparative results in terms of the mechanical properties, surface roughness, edge straightness, microstructural evolution, and finite element thermal analysis, the cross orientation of dual laser beam mode was recommended as the best choice to join coach peel panels.

The LWB joints are typically presented on the visible area of a car body for applications such as a deck lid or roof. Therefore, the final welded results not only should have the acceptable strength, but also, they should be defect free with highest surface quality to eliminate post-weld processing. In order to study the effect of laser welding-brazing process parameters on the weld quality, series of experiments were conducted in a systematic approach by means of design of experiments (DOE). RSM, as the well-known type of DoE design, was implemented to clarify the effects of input parameters on the final results. A comprehensive numerical

World Academy of Science, Engineering and Technology
International Journal of Materials and Metallurgical Engineering
Vol:11, No:12, 2017

simulation using commercial software ANSYS was proposed to study the thermal issues in the laser welding-brazing process. The captured heat distribution can define the fusion size on the welded side and obtained temperature history along the brazed interface can predict the growth of intermetallic layer.

II. MATERIALS, EXPERIMENTAL WORK AND FE MODELLING

A 4-kW fiber IPG laser was used for welding of Al6022 and Hot Dip Galvanized (HDG) low carbon steel in coach peel configuration, as shown in Fig. 1. The thickness of panels was 1.2 mm and 0.65 mm for aluminum and HGD, respectively. The selected filler wire was AA 4020 (AlSi3Mn1) with a diameter of 1.6 mm. The nominal chemical compositions of these two materials are given in Table I. To prevent the laser head from any possible damage from the beam reflection, the laser head was inclined to 5° with regards to the vertical axis. The dual laser beam mode was provided by a beam splitter mounted on the laser head to deliver two beams (side by side) with power ratio of 50/50. The weld surface was shielded by pure argon, with a flow rate of 25 SCFH under an inclination angle of 30° to the horizontal surface.
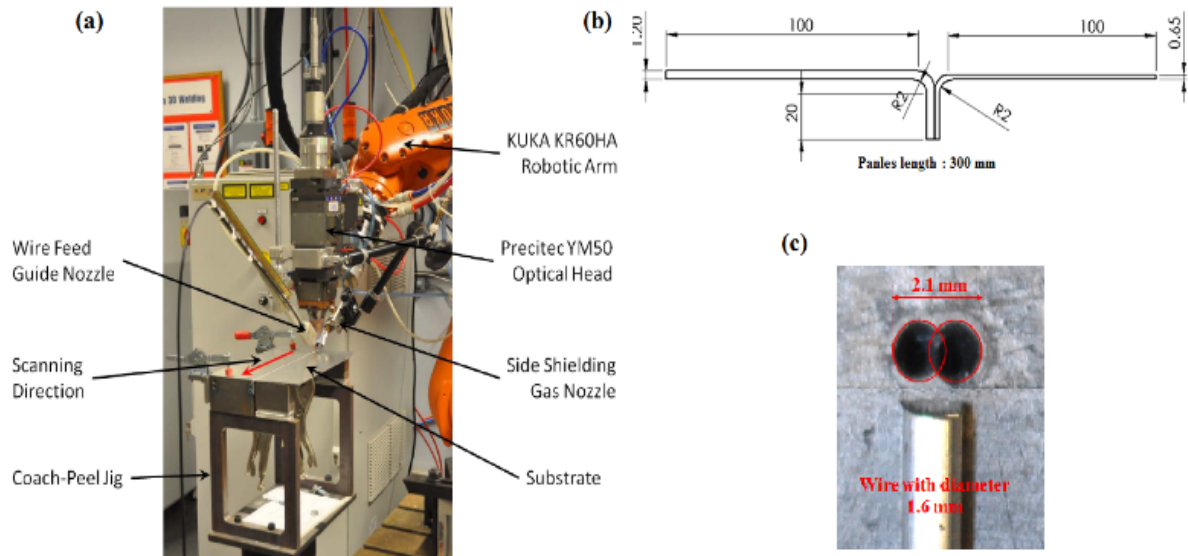

Fig. 1 (a) Schematic view of experimental setup, (b) dimensions of coupons c) dimension of dual laser beam

TABLE I
CHEMICAL COMPOSITION OF SUBSTRATE MATERIALS

Substrates	Alloying elements						
	Si	Fe	Mn	Mg	Zn	Ti	Al
Al6022	1.00	0.15	0.07	0.56	0.01	0.02	Bal.
Hot dip Galvanized steel (HDG)	C	Al	Mn	P	Si	S	Fe
	0.003	0.034	0.11	0.01	0.005	0.008	Bal.

The transversely cut joints were used to characterize the microstructure and intermetallic layer by means of optical microscopy and scanning electron microscopy (SEM) equipped with an energy dispersive spectroscopy (EDS). To conduct the mechanical tensile test, the coupons were cut by an abrasive waterjet cutting machine in order to meet the standard for the tensile-test sample ASTM E 8M-01 [10]. To validate the simulation results, the thermal cycle during the welding process was captured by a number of K-type thermocouples mounted close to the welded/brazed area. The National Instruments data acquisition system was used to capture the temperature at every 100 ms. Surface roughness of the beads was measured by Micro Photonic Nanovea non-contact profilometer.

To optimize the process parameters, a three-factor with three-level Box-Behnken design table was selected as given in Table II. The main processing parameters such as laser power, welding speed, and wire feed rate were selected as the independent input variables, and surface roughness and mechanical strength represented the output variables. The RSM approach offered the number of 17 experiments.

TABLE II
PROCESS VARIABLES AND EXPERIMENTAL DESIGN LEVELS

Variable (factors)	Unit	Notation	-1	0	1
Laser power	kW	LP	3.2	3.6	4
Welding speed	mm/s	WS	60	70	80
Wire feed rate	mm/s	WFR	70	80	90

The FEM was utilized to obtain the temperature history during the LWB process. The differential equation of thermal conduction was applied:

$$\rho \frac{\partial (C_p T)}{\partial t} = k \left(\frac{\partial^2 T}{\partial^2 x} + \frac{\partial^2 T}{\partial^2 y} + \frac{\partial^2 T}{\partial^2 z} \right) + \dot{q}_{laser}(x, y, z, t) \qquad (1)$$

where $\rho, C_p, $ T, t, k and x, y, z are the material density, specific heat, temperature, time, thermal conductivity, and Cartesian coordinates, respectively. For the moving heat source model, the laser induced volume heat source in the form of Rotary Gaussian was described by the following equation (Fig. 2) [11].

World Academy of Science, Engineering and Technology
International Journal of Materials and Metallurgical Engineering
Vol:11, No:12, 2017

$$\dot{q}_{laser}(cross\ beam) = \frac{9\eta Q}{\pi H R_0^2 (1-e^{-3})} \exp\left(\frac{-9}{R_0^2 \ln\left(\frac{H}{-y}\right)}\left((x - x_0 \pm d)^2 + (z - vt)^2\right)\right) \quad (2)$$

where η is the absorption coefficient, Q is the nominal power of the laser beam, y varies from 0 to H, H is the depth of the fusion zone, v is the welding speed, R_0 is the effective radius of the volumetric heat source on the material surface, and d is

the center distance of dual beams. The dimensions of FE model of dissimilar LWB joint are shown in Fig. 2. The element type was SOLID70 for meshing the model, and the size of the elements were modified to get independent results from element size. The steps of the simulation process are shown in Fig. 3. The "kill and birth" technique was implemented in the FE model to mimic the nature of adding filler material during the joining process.
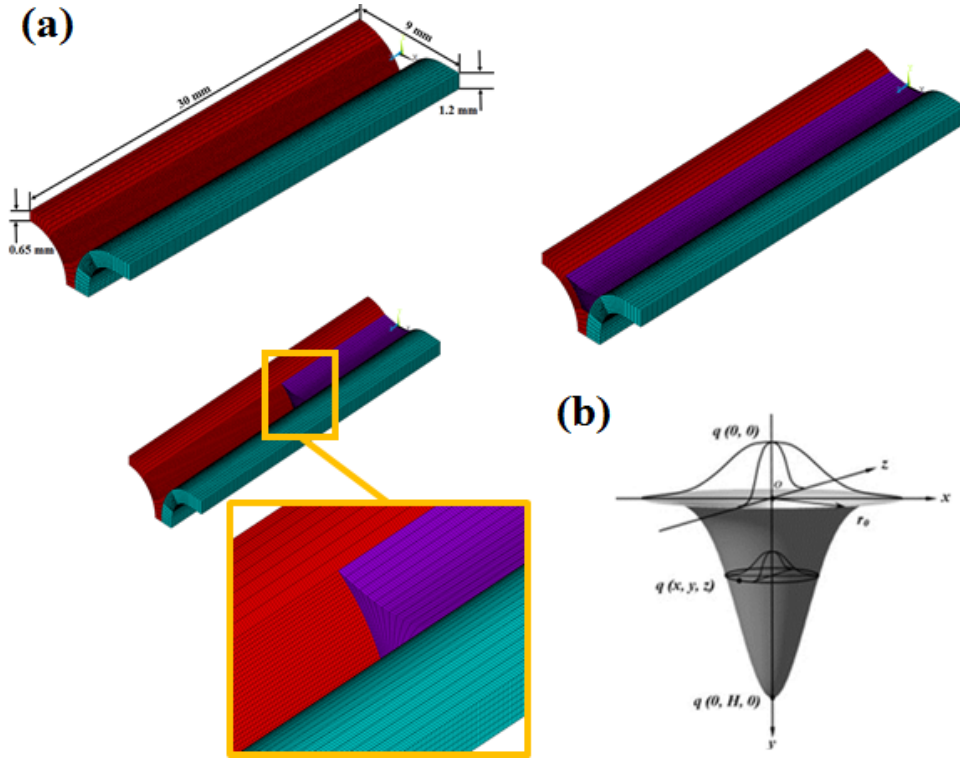

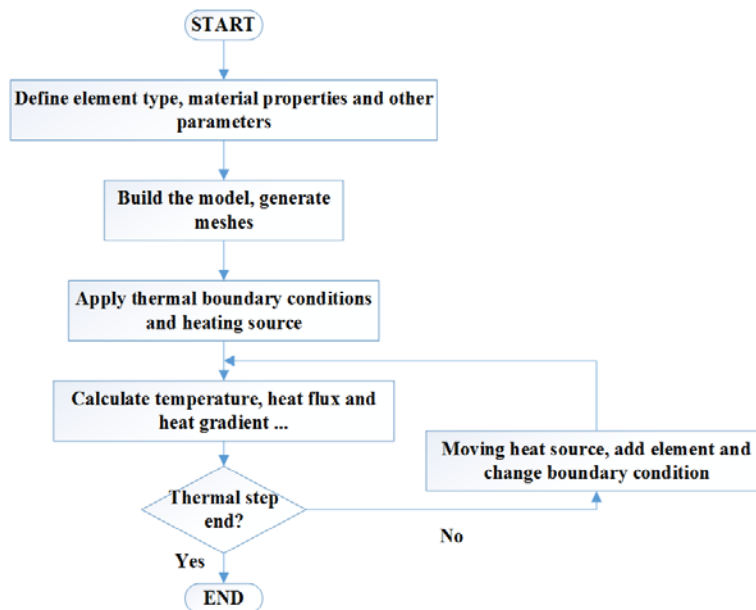Fig. 2 (a) Finite element meshed model (b) Rotary Gaussian body heat source [11]

Fig. 3 Flow chart of numerical procedure

World Academy of Science, Engineering and Technology
International Journal of Materials and Metallurgical Engineering
Vol:11, No:12, 2017

III. PARAMETERS OPTIMIZATION

In order to correlate the minimum surface roughness and maximum tensile load to the process parameters in the weld bead, second order polynomial function were utilized to fit the experimental results. The possible functions for the interest responses of LWB joints, the responses R, surface roughness and mechanical strength could be defined as functions of laser power (LP), welding speed (SS), and wire feed rate (WFR).

$$R = \alpha_0 + \alpha_1(LP) + \alpha_2(SS) + \alpha_3(WFR) + \alpha_{12}(LP.SS) + \alpha_{13}(LP.WFR) + \alpha_{23}(SS.WFR) + \alpha_{11}(LP^2) + \alpha_{22}(SS^2) + \alpha_{33}(WFR^2) + e_r \qquad (3)$$

where α_0 is constant coefficient, α_i, α_{ij} and α_{ii} are coefficients of linear, interaction and quadratic terms.

Design-Expert V10 statistical software was used to analysis the measured responses. The step-wise regression method was utilized to exclude the insignificant terms with respect to their p-values. Since in this study, the level of confidence was scheduled to be 95%, therefore insignificant terms should have p-value more than 0.05. The final mathematical response models for mechanical resistance and surface roughness as described by design expert software are summarized in (4) and (5).

Resistance = 2981.687-1154.918×LP-3.803×SS-17.287×WFR + 0.907×LP×SS + 4.758×LP×WFR + 101.953×LP² (4)

Surface roughness = 234.64 – 135.97×LP + 0.189×SS – 3.306×WFR – 0.0607×LP×SS + 1.891×LP×WFR – 0.00137×SS×WFR + 19.34×LP2 + 0.00106×SS2 (5)

In order to study the spread of the predicted results versus the experimentally measured ones, the values were plotted in a scatter graph that is depicted in Fig. 4. As it is evident, there are good agreements between the estimated and measured data with the trendline slope of almost 1 for two responses.

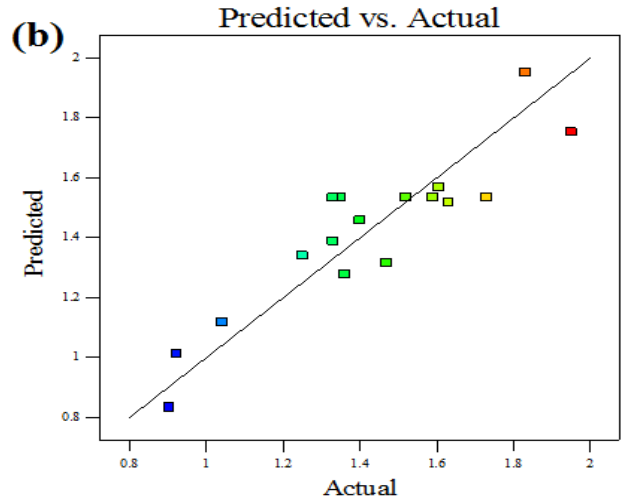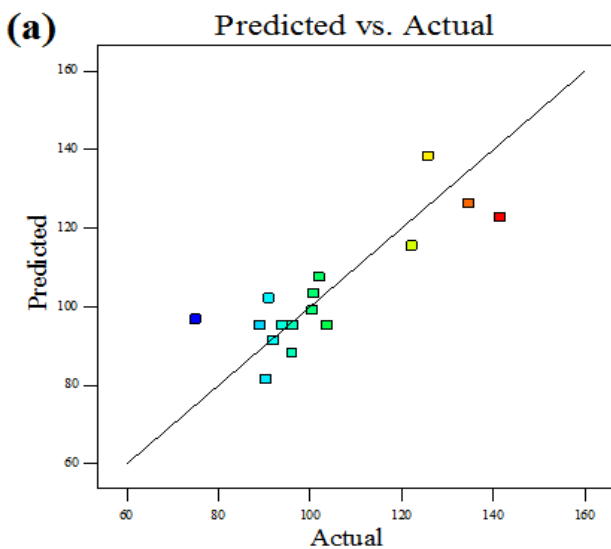(a) Predicted vs. Actual

(b) Predicted vs. Actual

Fig. 4 The relation between the calculated and measured results for (a) mechanical resistance and (b) surface roughness
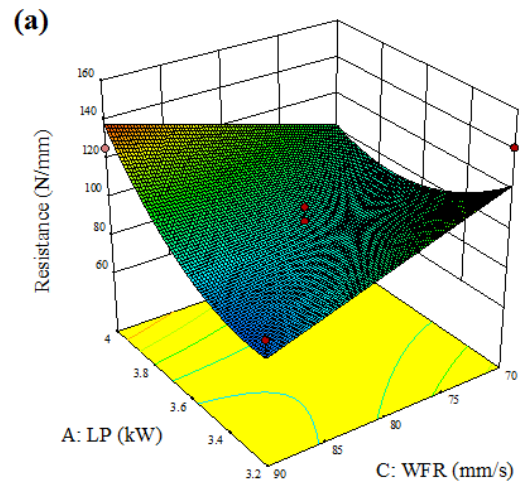
TABLE III
THE ANOVA TABLE FOR MECHANICAL RESISTANCE

Factor	Sum of Squares	Mean Square	F-value	p-value	
Model	3578.05	596.34	4.08	0.0248	Sign.
Residual	1460.89	146.09			
Lack of fit	1346.79	224.47	7.87	0.0329	Sign.
Total	5038.95				

TABLE IV
THE ANOVA TABLE FOR SURFACE ROUGHNESS

Factor	Sum of Squares	Mean Square	F-value	p-value	
Model	1.21	0.14	7.78	0.0084	Sign.
Residual	0.13	0.018			
Lack of fit	0.012	4.15E-3	0.15	0.9262	Not Sign.
Total	1.38				

As the basic feature of RSM, the interaction effects of process parameters on surface roughness and mechanical resistance are presented in 3D response surfaces (Fig. 5). It is evident that, by increasing the wire feed rate and scanning speed, the surface roughness was also enhanced.

(a)

World Academy of Science, Engineering and Technology
International Journal of Materials and Metallurgical Engineering
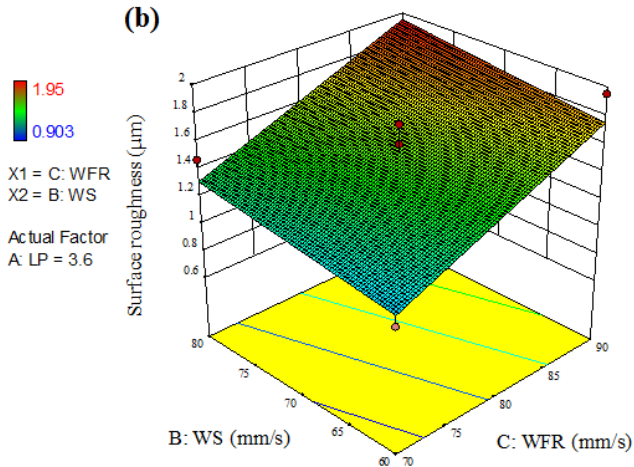Vol:11, No:12, 2017

Fig. 5 Response surface (a) effect of lase power and welding speed on resistance (b) effect of wire feed rate and scanning speed on surface roughness

Since the ultimate goal in this study is minimizing the surface roughness and maximizing the mechanical strength, the optimization process should follow the multi-response approach. In multi-response optimization method based on RSM regression models, the desirability function with respect to the output responses was defined. This function alters the characteristic of the multi response state to a single dimensionless factor called desirability factor. The desirability function can be expressed as (6) [12]. The numerical

optimization for Box-Behnken design offered the optimal experimental condition with highest desirability value of 0.92 listed in Table V. In order to validate the accuracy of multi-objective optimization results, additional experiments were conducted at the optimum condition.

$$Desirability = \left[\prod_{j=1}^{N} d_i^{ri} \right]^{1/\Sigma ri} \qquad (6)$$

TABLE V
NUMERICALLY OBTAINED OPTIMAL PROCESSING CONDITION

Processing parameters				Responses	
LP (kW)	WS (mm/s)	WFR (mm/s)		Resistance (N/mm)	Surface roughness (µm)
3.2	60	70	Measured	120.34	0.93
			Predicted	131.78	0.91

IV. RESULTS AND DISCUSSION

The obtained optimum processing parameters were applied in the FE model as follows: the laser power Q was 3.2 kW, welding speed was 60 mm/s, and effective radius of heat source on the bead surface r_0 was 2.5 mm. The numerically-obtained temperature history of LWB process by dual laser cross-beam mode is depicted in Fig. 6. The asymmetry shape of thermal counter attributed to the difference in thermal conductivity of panels in which aluminum with higher one could conduct the heat better than steel.
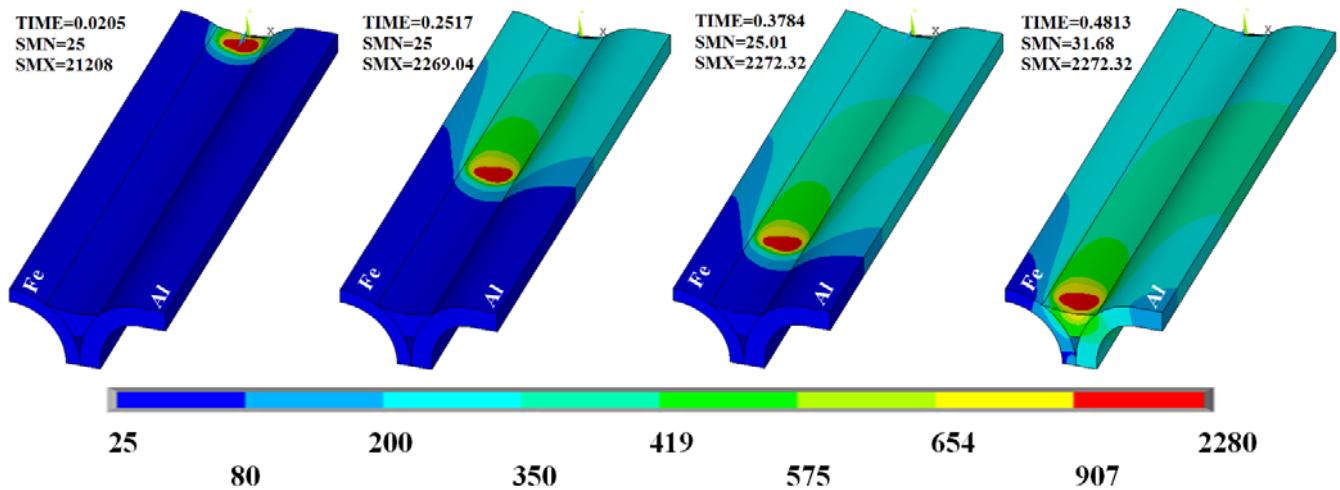

Fig. 6 Temperature field history at different times

The maximum temperature obtained at all processing times (2280 °C) was far lower than the boiling temperature of steel (2800 °C). By comparing the experimentally measured temperatures around the weld and the numerical ones, the accuracy of introduced model for thermal simulation conducted can be verified. Furthermore, cross-sectional views of the experimentally welded joints and numerically determined confirm the consistency of FE model (Fig. 7).

The common type of defect in joints with galvanized steel substrates is the gas pore with the potential source of zinc

evaporation from galvanized coating. This phenomenon can be more important in laser-based joining processes at high welding speeds with an inadequate amount of time for zinc vapors to escape [13]. Fig. 7 shows that the isotherm at the melting temperature of zinc (419 °C) reached the molten pool boundary at the surface, whereas the isothermal surface at the boiling temperature of zinc (907 °C) was restrained in the upper section of the molten pool away from the steel surface. This simulation result can confirm the fact that the zinc layer was only able to dissolve into the molten pool, and the

World Academy of Science, Engineering and Technology
International Journal of Materials and Metallurgical Engineering
Vol:11, No:12, 2017

possibility of boiling the zinc layer was eliminated by employing the optimized processing parameters.
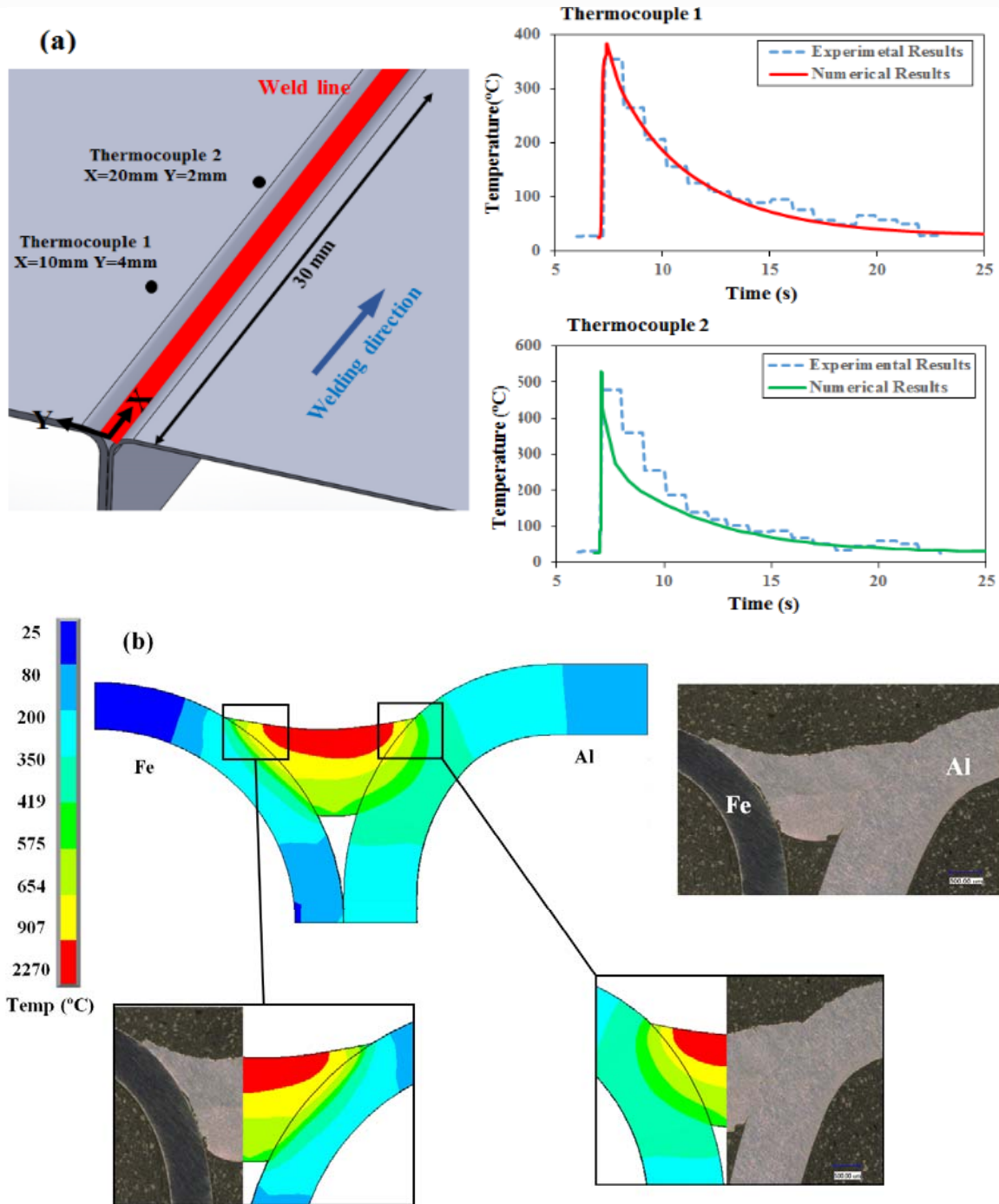

Fig. 7 Validation of simulation results by comparing (a) the thermal cycles and (b) the weld shape

As earlier mentioned, the nature of IMC growth is time and temperature dependent process. Bouche et al. [14] proposed a kinetic model to explain the mechanism of IMC growth between solid iron and molten aluminum and identified the temperature range of 700–900 °C to grow Al_5Fe_2 phase. The thermal history at interfacial area (Fig. 8) can clarify that, at that temperature range, aluminum was in the liquid state. The wetting time at the molten aluminum-solid steel interface was less than 1 s and was not sufficient enough for thickening IMC. These thermal cycles were very short with sharp thermal loadings which leads to generation of thin IMC layers in LWB process. The maximum thickness of IMC layer was measured at the middle section of interface around 5 μm for the optimum processing condition which was far from the literature reported critical value (10 μm) (Fig. 9).

It is a proven fact that thicker IMC layer jeopardizes the

strength of joint and may cause the fracturing from this brittle layer. Since the thickness of LWB joints in optimal processing condition with AlSi3Mn1 filler wire was thinner, Fe/Al interface was not the weakest part of joint and failure was occurred at the fusion side as shown in Fig. 10. In failure mechanism of LWB joints, crack was initiated and then propagated along the interface of weld/braze bead and aluminum substrate. With the continued elongation, the coach peel samples will bend, that alters the loading conditions. The crack tip propagated into the welded/brazed bead along the growth direction of the columnar dendrites, moved through the interdendritic region and ended with full fracture.

The other experimental observation that was also validated by FE results was the presence of non-uniformity of intermetallic layer. Yang et al. [15] and Fillard et al. [8] detected this kind of phenomena in the experimental observations as well. They proved that the thickest IMC layer was generated in the middle section of brazing interface. As seen in Fig. 8, the sections at the Fe/Al interface, denoted by points C and D, experienced the higher temperature than the other points. This higher temperature and longer duration time at critical temperature range can lead to generate the thicker IMC layer than in the other sections.

V. CONCLUSIONS

The following conclusions can be drawn from the current study:

1. The Box-Behnken statistical design accompanied with the RSM was a simple and efficient way to study the effect of process parameters and their interactions on the defined responses.
2. The multi-response optimization approach by considering the minimum surface roughness and maximum mechanical strength has determined the optimal process parameters of 3.2 kW for laser power, 60 mm/s for welding speed, and 70 mm/s for wire feed rate.
3. A comprehensive FE model was developed to study the temperature field of LWB joint.
4. The dual cross laser beam mode can be used to join aluminum and galvanized steel at high processing speed. The generated IMC layer in the middle section of brazing interface as the thickest part, was less than 5 µm.
5. In the tensile test, the fracture took place at the aluminum side rather than at the interface between the weld bead and the steel side.
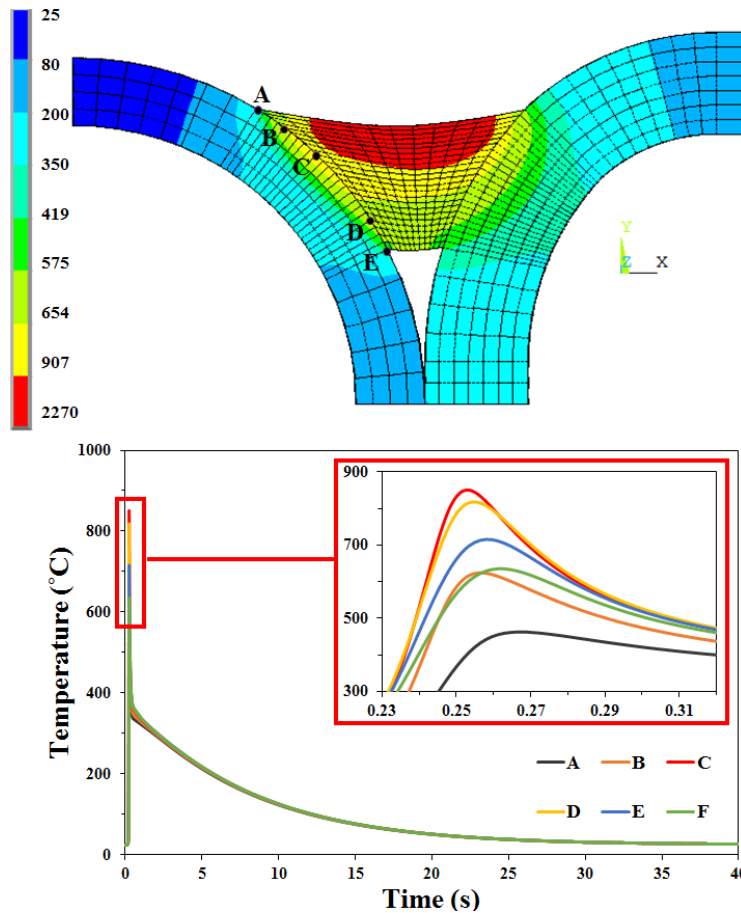

Fig. 8 Temperature histories at different locations along the brazing interface

World Academy of Science, Engineering and Technology
International Journal of Materials and Metallurgical Engineering
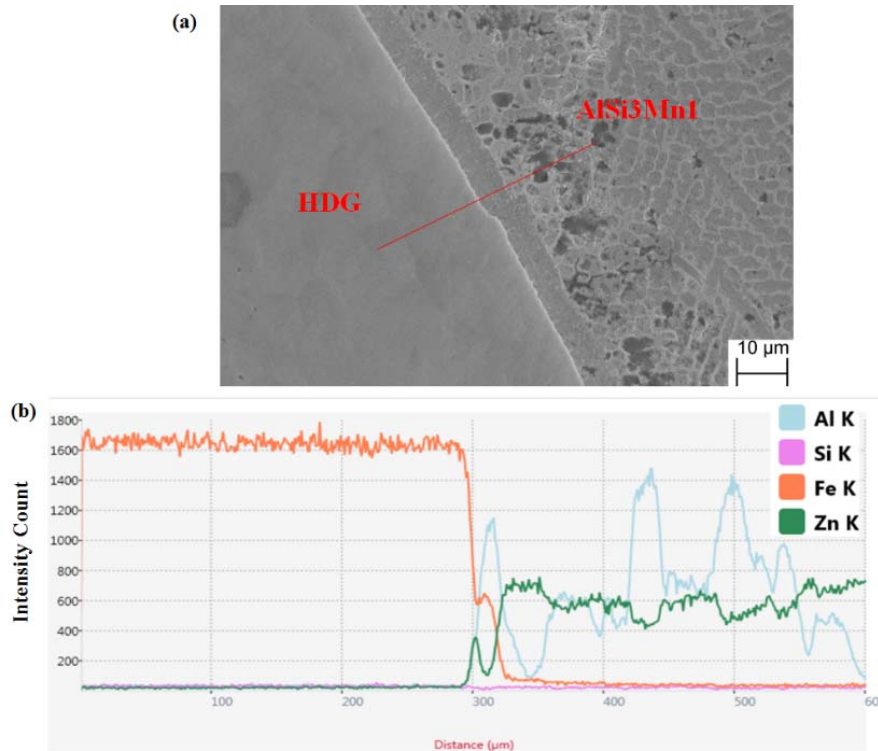Vol:11, No:12, 2017

Fig. 9 (a) SEM micrographs and (b) distribution of alloying elements at the Fe/Al interface
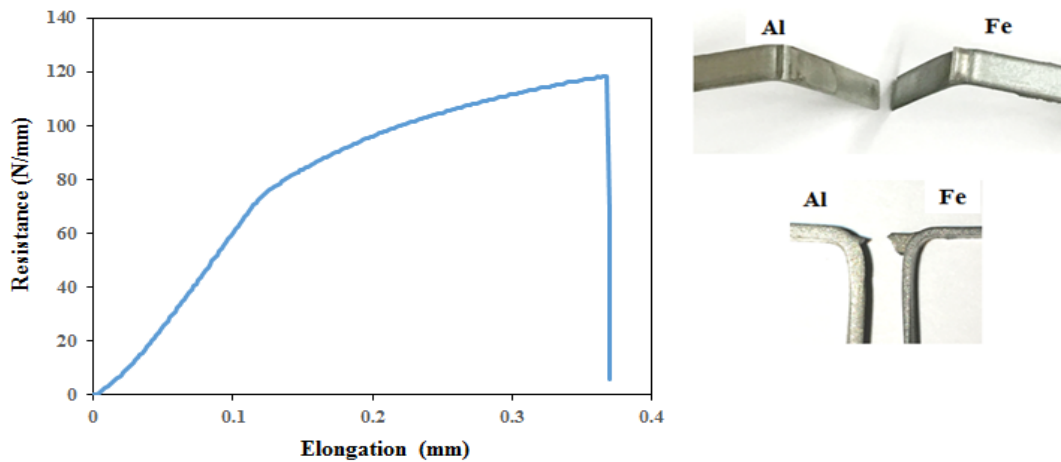
Fig. 10 Tensile test curve and fractured sample for coach peel LWB joint

REFERENCES

[1] K, Martinsen, S. Hu, B.E. Carlson, "Joining of dissimilar materials. CIRP Annals" *Manufacturing Technology*. 64, 2015, pp. 679-99.
[2] Y. Yao, J. P. Meng, L. Y. Ma, G. Q. Zhao, L. R. Wang, "Study on Hot Stamping and Usibor 1500P" *Applied Mechanics and Materials*, Vol. 320, 2013, pp. 419-425.
[3] S. Meco, G. Pardal, S. Ganguly, S. Williams, N. McPherson, "Application of laser in seam welding of dissimilar steel to aluminium joints for thick structural components" *Optics and Lasers in Engineering*, vol. 67, 2015, pp. 22-30.
[4] D. Zhou, S. Xu, L. Zhang, Y. Peng, J. Liu, "Microstructure, mechanical properties, and electronic simulations of steel/aluminum alloy joint during deep penetration laser welding" *The Int. Journal of Advanced Manufacturing Technology*, Vol. 89, 2017, pp 377–387.
[5] M. Rathod, M. Kutsuna, "Joining of aluminum Alloy 5052 and low-carbon steel by laser roll welding" *Welding Journal*, 2004, vol.83, pp 16S-26S
[6] E. Schubert, M. Klassen, I. Zerner, C. Walz, G. Sepold, "Light-weight structures produced by laser beam joining for future applications in automobile and aerospace industry" *Journal of Materials Processing Technology*, 2001, vol. 115, pp 2-8
[7] J. Lin, N. Ma, Y. Lei, H. Murakawa, Shear strength of CMT brazed lap

World Academy of Science, Engineering and Technology
International Journal of Materials and Metallurgical Engineering
Vol:11, No:12, 2017

joints between aluminum and zinc-coated steel. *Journal of Materials Processing Technology,* 2013, vol. 213, pp 1303-1310.

[8] G. Filliard G, M. Mansori , L. Tirado, S. Mezghani, C. Bremont, M. Metz-Noblat, "Industrial fluxless laser weld-brazing process of steel to aluminium at high brazing speed" *Journal of Manufacturing Processes*, 2017, vol. 25, pp 104-15.

[9] M. Mohammadpour, N. Yazidan, G. Yang, H. P. Wang, B. Carlson, "Effect of dual laser beam on dissimilar welding-brazing of aluminum to galvanized steel" *Optics & Laser Technology*, 2018, vol. 98, pp 214-228

[10] Annual book of ASTM standards, "metals test methods and analytical procedures" *ASTM International*, vol. 03, 01. 2003.

[11] J. Ma, F. Kong, R. Kovacevic, "Finite-element thermal analysis of laser welding of galvanized high-strength steel in a zero-gap lap joint configuration and its experimental verification" *Materials and Design*, 2012, vol. 36, pp 348–358.

[12] Montgomery, D. C., Montgomery, D. C.: "Design and analysis of experiments" *Wiley*, Vol. 7, New York, 1984.

[13] A. M. Milani, M. Paidar, A. Khodabandeh, S. Nategh, "Influence of filler wire and wire feed speed on metallurgical and mechanical properties of MIG welding–brazing of automotive galvanized steel/5754 aluminum alloy in a lap joint configuration" *The Int. Journal of Advanced Manufacturing Technology*, 2016, vol. 82, pp 495-506.

[14] K. Bouché, F. Barbier, A. Coulet, "Intermetallic compound layer growth between solid iron and molten aluminium" *Material Science Engineering A*, 1998, vol. 249, pp 167-175.

[15] G. Yang, M. Mohammadpour, N. Yazdian, J. Ma, B. Carlson, H. P. Wang, "Cross-Beam Laser Joining of AA 6111 to Galvanized Steel in a Coach Peel Configuration" Lasers in Manufacturing and Materials Processing, 2017, vol. 4, pp 45-59.

Masoud Mohammadpour is a PhD student at the Research Center for advanced Manufacturing (RCAM) at Southern Methodist University. He received his M.S. in Mechanical Engineering with a focus on fatigue life studies of FSSW aluminum 7075-T6 joints at Urmia University, Iran in 2012. His current field of research includes laser welding of lightweight materials and hybrid laser-arc welding for similar and dissimilar joints with the purpose of optimized and improved quality of weld.

Blair Carlson, Ph.D., is a lab group manager at General Motors Research and Development in Warren, Michigan. He received his Ph.D. in Materials Science at University of Michigan. He has worked as an Advanced Manufacturing Manager at SAAB and as a Senior Engineer at General Motors.

Radovan Kovacevic, Ph.D., is Herman Brown Chair Professor of Mechanical Engineering and the Director of Research Center for Advanced Manufacturing and Center for Laser-Aided Manufacturing. He is a Fellow of the American Society of Mechanical Engineering, Society of Manufacturing Engineering, and American Society of Welding Engineers. He has to his credit over 600 technical publications and seven US Patents.